

**DETAILED EXPERIMENTAL DATABASE OF DENT & GOUGE DEFECTS
TO QUALIFY BURST AND FATIGUE STRENGTH MODELS**

Main author

M. Zaréa¹

France

Co-authors

R. Batisse¹, B. Leis², P. Cardin¹

France, USA

¹*GDF SUEZ – Research & Innovation Division, CRIGEN, 361 avenue Président Wilson, 93 211 Saint-Denis-la-Plaine, France*

²*Battelle Memorial Institute, Columbus Ohio, USA*

1. ABSTRACT

Mechanical Damage on gas and oil transmission pipelines is the major single cause of incidents with leaks in the Europe and USA as identified in the EGIG and PHMSA incident databases. Mechanical damage in buried pipelines can occur due to a number of causes; particularly, dent and gouge defects are due to ground working machinery strike, rock strikes during backfilling, amongst others. The long-term integrity of a pipeline segment damaged by a dent and gouge defect is a complex function of a variety of parameters, including pipe material properties, pipe geometry, defect geometry linked to indenter shape, indenter support, aggression conditions.

The complexity and extreme variability of these dent and gouge defect shapes lead simple assessment models to scattered predictions, hinting towards an insufficient description of real structural and material behavior. To improve knowledge beyond the numerous studies led in the past, and to provide a sound foundation for developing and validating mechanistic models for predicting burst and fatigue strength of such defects, a large experimental program was funded by PRCI and US DoT as well as coordinated with a complementary EPRG program.

The experimental test program consists of two related PRCI projects (MD 4-1 and MD 4-2), that share the material characterization work on modern pipe steel grades, X52 and X70, and of the DoT project #DTPH56-08-T-000011 (the DoT project) aimed at testing vintage pipes.

- MD 4-1 (modern pipe) and the DoT project (vintage pipe) is focused on experimental study of realistic combined “Dent and Gouge” defects with different “bracketing features”, submitted to full scale burst and fatigue tests, in addition to extensive characterization.
- MD 4-2 (modern pipe) and the DoT project (vintage pipe) concerns plain dents, dents interacting with girth and seam welds, and dents interacting with metal loss features where the dents are pressure cycled until fatigue failure.

This paper gives an overview of some of these activities: material characterization, full scale tests on Dents with Gouges (PRCI project MD 4-1) as well as associated detailed explanations about first approaches in modeling fatigue life of dents combined with gouges, (PRCI project MD 4-4).

The final outcome of the expected knowledge improvements about the mechanical strength of dent and gouge combinations will be applicable by pipeline operators, in order to enhance safety for the general public as well as operating personnel.

TABLE OF CONTENTS

1. Abstract
2. Introduction
3. Material Characterization
4. Tests on Dents with Gouges
5. Current Approach in Fatigue Modeling for Dent and Gouge Defects
6. Conclusion
7. Acknowledgements
8. References

2. INTRODUCTION

Mechanical damage on gas and oil transmission pipelines is the major single cause of incidents with leaks in the USA and Europe as identified in the EGIG [1] and PHMSA [2] incident databases. Mechanical damage defects result from direct contact with the pipe and are due to a number of causes; the pipe resting on rock, ground working machinery strike, rock strikes during backfilling, amongst others. We focus here on the leading case, i.e. external interference, producing in general dents associated with gouges. The long-term integrity of a dented and gouged pipeline segment is a complex function of a variety of parameters, including pipe material properties, pipe geometry, indenter shape, defect geometry, indenter support & velocity, and pressure history at and following indentation. In order to estimate the safe remaining operational life of a pipeline with mechanical damage defects, all of these factors must be accounted for in the analysis.

The complexity and extreme variability of dent shapes lead simple assessment models to uncertain predictions, hinting towards an insufficient description of real structural and material behavior. The prediction scatter increases even more when a dent is associated with a secondary feature as those listed above, because the complexity increases even more.

In order to improve knowledge beyond the numerous studies led in the past, and to provide a sound foundation for developing and validating mechanistic models for predicting burst and fatigue strength of such defects, a large experimental program was funded by PRCI and US DoT. This research program collects more detailed and comprehensive experimental data to facilitate the improvement of mechanical damage assessment models for dents with other features: gouges, metal loss and welds.

The experimental tests program consists in two related PRCI projects (MD-4-1 and MD-4-2) that share the material characterization work on modern pipe steel grades, X52 and X70, and in the DoT project # DTPH56-08-T-000011 (the DoT project) aimed at testing vintage X52 grade:

- MD-4-1 (modern pipe), its extension MD-4-6, and the DoT project (vintage pipes) share the same approach for Dent and Gouge damage: creation of three similar samples of realistic Dent and Gouge defects with different sizes of combined dent and gouge. Realistic defect creation means the pipe is hit with an excavator-like Pipe Aggression Rig fitted with an excavator tooth so that gouge and dent are created simultaneously. Two samples are used for burst and fatigue tests with very detailed instrumentation. After failure, a thorough failure investigation highlights the failure mechanisms and the issues of crack initiation and propagation. The third sample is used for detailed characterization, in terms of geometry, of residual stresses, presence or absence of microcracks, etc. Tests are performed by GDF SUEZ' Research and Innovation Division, CRIGEN, France.
- MD-4-2 (modern pipe), and the DoT project(vintage pipe): full scale dent test results, that encompasses plain dents, dents interacting with girth and long seam welds, and dents interacting with metal loss features, in both the unrestrained and restrained condition where the dents are pressure cycled until a fatigue failure occurs in the dent. This project is not detailed here.

This paper shows the test matrix, test conditions and representative results from burst and fatigue tests on dent and gouge defects on modern steel pipes from the MD-4-1 project.

On the modeling side, it details ongoing efforts to develop improved pipeline dent and gouge fatigue integrity assessment models underway in PRCI project MD-4-4. Modeling of fatigue failure is performed by Battelle Memorial Institute, Ohio, USA. The companion PRCI project MD-4-3 dealing with improved modeling of dent and gouge burst strength is not reported here. It should also be mentioned that this effort is coordinated with EPRG, that manages two complementary projects on burst strength of dents with gouges.

3. MATERIAL CHARACTERIZATION

Two different pipes are currently being used in the full scale test program and are identified as Pipes A and B. Pipe A and B are modern materials of Grades X-52 and X-70 respectively. Their outer diameter is 609.6 mm diameter. The nominal thicknesses of Pipes A and B C are 7.9 mm and 8.89 mm respectively. All the joints from pipes A and B came from the same heats. Pipe A and Pipe B have been used in both the MD 4-1 and 4-2 programs. A vintage pipe will be used in the MD 4-1 program to start extending coverage of results also to existing steel grades.

3.1 Baseline Material Characterization

Detailed material characterization tests were carried out on the two pipes and included chemical analysis, microstructure evaluation, tensile tests, Charpy impact testing and CTOD testing and are detailed in Tables 2.1 - 2.5 respectively. These are **modern, clean, strong and tough steels**.

Composition (wt%)	Pipe A	Pipe B
C	0.04	0.04
Mn	0.83	1.60
S	<0.005	0.007
P	0.008	0.007
Si	0.23	0.16
Cu	0.21	0.27
Ni	0.13	0.13
Cr	0.07	0.07
V	0.006	<0.005
Cb	0.023	0.071
Sn	0.008	0.008
Mo	0.054	0.198
Al	0.038	0.049
Ca	<0.005	<0.005
B	<0.002	<0.002
Ti	<0.005	0.020
N	0.013	0.010

Table 2.1: Chemical Analysis Results for the two Pipes

Pipe ID	Inclusion Volume Fraction (%)	Pearlite Volume Fraction (%)	Ferrite Grain Size (µm)
A	0.05	3.2	6.2
B	0.07	3.1	3.2

Table 2.2: Quantitative Metallographic Test Results for the two Pipes

Pipe ID	Orientation	0.5% Yield Strength (MPa)	Ultimate Strength (MPa)	% Elongation
A	Transverse	437	516	35
	Longitudinal	450	503	34
B	Transverse	506	667	23
	Longitudinal	546	652	30

Table 2.3: Pipe Body Tensile Strip Test Data for the two Pipes

3.2 Additional investigation of the hardened layer observed on defect 2.1.3

Pipe ID	Specimen Size	Upper Shelf Impact Energy, Joules (Average)
A	2/3	160
B	2/3	87

Table 2.4: Base Metal Charpy V-Notch Impact Test Results of the two Pipes

Pipe ID	CTOD @ -5°C (Total) (mm)	Failure Type
A	0.506	δ_m
B	0.329	δ_m

Table 2.5: Base Metal CTOD Test Data of the two Pipes

It was systematically observed that after dynamic impacts, a distinctly hardened outer layer and a strain hardened layer beneath it were created at the gouge surface as shown in Figure 3.2.1.

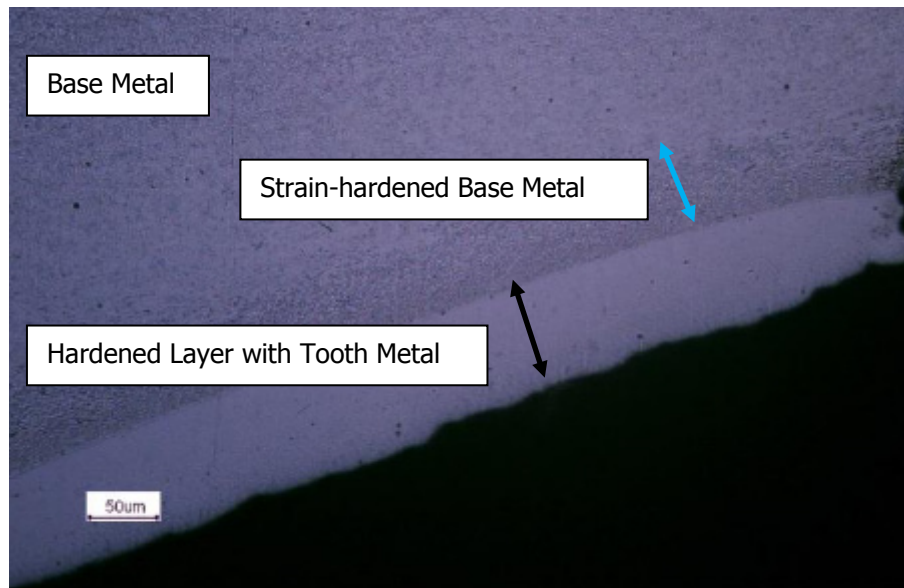


Figure 3.2.1 : Hardened layer at gouge surface of defect 2.1.3

The outer layer is most often between 50µm and 100µm thick and its hardness is very high, around 600 HV0.5. Initially, it had been assumed that the pipe steel turned into a martensitic phase due to the sudden thermal cycle due to the tooth impact – very quick friction heating followed by rapid conductive cooling in a thin layer.

Such high hardness values were not expected, so to check the initial assumption, additional investigations were carried out: several thermal tests were performed with a Gleeble furnace to reproduce this martensitic microstructure of the pipe steel. But it was not possible to reproduce such hardening, and the highest hardness achieved was around 275 HV, far below 600 HV. Alternatively, we used the Blondeau formula giving the martensitic hardness versus the chemical steel composition and cooling speed “tr” between 800°C and 500°C :

$$HV=127+949 * \%C+27 * \%Si+11 * \%Mn+8 * \%Ni+16 * \%Cr+21 * \log(tr)$$

Using the pipe steel chemical composition and estimating conservative cooling rates between 1°C/s and 5°C/s, the calculated hardness results are between 200HV and 220HV. The reason is that the carbon content is too low to produce a hard martensitic microstructure. This calculation confirms the fact that the hardened layer is not pure pipe steel.

In order to investigate further, a tooth used for impact tests was analyzed (Figure 3.2.2).



Figure 3.2.2: **Samples taken from a tooth for chemical and hardness analysis**

Chemical and hardness analysis were performed on tooth samples and compared to the hardened layer characteristics. Hardness values are close (535 HV for the tooth and around 600 HV for the hardened layer). The chemical contents in table 3 show comparable values for the tooth and the hardened layer and differences with pipe steel concerning Silicium, Chromium and Manganese.

	%Si	%Cr	%Mn
Hardened layer	0.63	0.63	1.54
Tooth	0.64	0.63	1.49
Pipe steel	0.25	0.09	2.2

Table 3 : Comparison of chemical contents between hardened layer, tooth and pipe steel

These results open the way to the interpretation of the creation of the hardened layer from the tooth material. But this interpretation has to be confirmed by a relevant detailed description of the deposition mechanism due to friction mechanical and thermal effects between the tooth and pipe steel during the impact. In summary, **dynamic impact creates a very hard thin outer layer**, and a **strain hardened layer below**, both around **50 – 100 µm deep**.

Metallurgical investigation after defect creation indicates that **micro-cracking is associated with the outer layer**.

3.3 Cyclic behavior and influence of pre-strain on toughness

Dent creation leads to local inverse pipe bending. In this area, the load history is not monotonic with local plastic compression or tension strains occurring during dent creation and then reversing to the opposite sign during re-rounding due to internal pressure after removing the indenter. So there is a load history dependence of flow properties [3] associated with mechanical dent damage which could be taken into account by a material kinematic hardening law. In addition, the local plastic pre-strain induced by dents may significantly affect material toughness [3 - 6].

For this reason, cyclic behavior tests and toughness tests - J-Curves with pre-strain - were performed on the modern X52 and X70 materials. Figure 2.6 presents examples of results of the cyclic behavior and of the effect of pre-strain on modern X52 material.

A **slight kinematic effect** on mechanical behavior is observed with an elastic area increasing in tension and decreasing in compression with increasing strain.

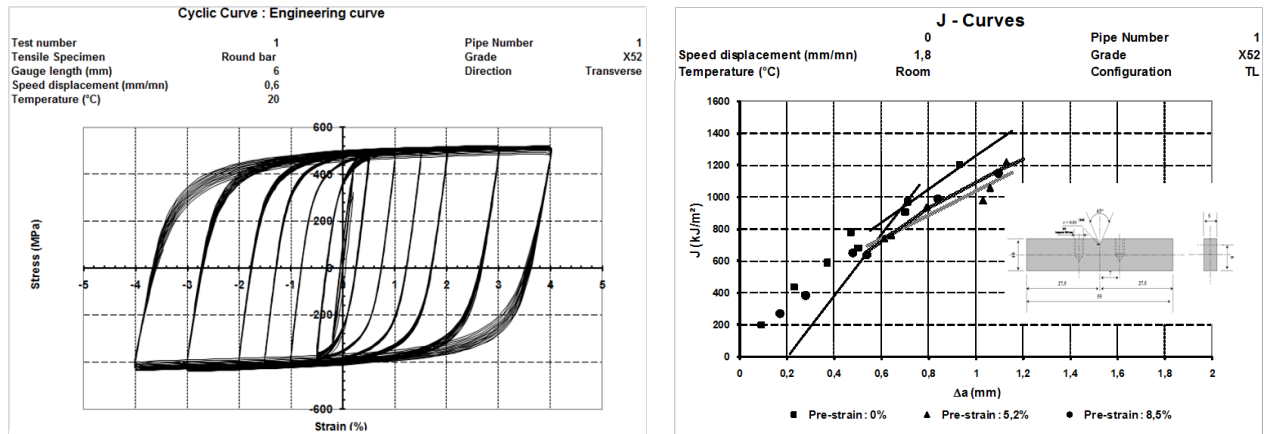


Figure 2.6: Cyclic behavior (left) and pre-strain effect up to 8.5% on toughness in modern X52 material (right).

Up to a 8.5% pre-strain, the high toughness level ($J_c = 929 \text{ kJ/m}^2$ without pre-strain) is not significantly affected ($J_c = 668 \text{ kJ/m}^2$ with 8.5% pre-strain) for this highly ductile modern material. The same behavior was found for the modern X70 material, therefore the influence of pre-strain on toughness should be more significant in less tough and clean steels.

4. TEST ON DENTS WITH GOUGES

Fifteen realistic combined Dent and Gouge defects were created with the Pipe Aggression Rig (Fig. 4.1.a) in modern pipes X52 and X70 in the frame of the MD 4-1 PRCI project and twelve more are planned to be created on vintage pipes in the DoT and MD 4-6 projects. The sizes of the defects were derived from an interpretation of defect dimensions found in the field, by favoring 'bracketing' configurations, i.e. extreme conditions, either highly dynamic impact or slower dynamic impact, resulting in different types of defects.

4.1 Tests matrix and global results

The experimental study is described in the matrix in Table 4.1.

Pipe number	MD 4-1 Project				MD 4-6 Project		DoT#339		
	Pipe 1 Modern X52		Pipe 2 Modern X70		Pipe 3 Vintage		Pipe 4 Vintage		
Type of defect	1	2	3	1	2	1	2	1	2
Destructive characterization	1.1.1	1.2.1	1.3.1	2.1.1	2.2.1	3.1.1	3.2.2	4.1.1	4.2.1
Burst test	1.1.2	1.2.2	1.3.2	2.1.2	2.2.2	3.1.2	3.2.2	4.1.2	4.2.2
Fatigue test	1.1.3	1.2.3	1.3.3	2.1.3	2.2.3	3.1.3	3.2.3	4.1.3	4.2.3

Table 4.1: Test matrix for combined Dent and Gouge defects - MD 4-1, DoT#339 and MD 4-6.

Defects are identified by three characters x.y.z :

- x.y.z: x identifies the pipe number x;
- x.y.z: y identifies the type of combined defect (shallow dent and moderate gouge, severe gouge, severe dent with moderate gouge, etc., and may change from one pipe to another);
- x.y.z: z identifies the defect number for each type (1 for destructive characterization, 2 for burst test, 3 for fatigue test).

Currently the MD-4-1 project on modern pipes is in its finalization stages, whereas the work on vintage pipes (MD-4-6 and DoT projects) is in its early phases.

Each mechanical strength test is particularly well instrumented:

- During **defect creation** in highly dynamic or slower dynamic conditions with realistic indenter impact (tooth from excavator), forces and displacements are recorded in horizontal and vertical directions to evaluate defect creation energy versus time. Strain gauges are stuck on the internal pipe wall to record strains during indenter impact.
- For **fatigue and burst tests**, a wide range of instruments are used, like strain gauges (rosettes) around the gouges, opening displacement gauge: specifically for fatigue tests: LVDT, potential drop sensor, pictures of targets recorded with a camera synchronized with the pressure to record defect evolution with fatigue cycles, and a specific profiling tool to record the evolution of the longitudinal dent profile during the monotonic pressure increase.

After defects creation, 3D laser mapping is performed to record the defect geometry and cracks are searched for by M.P.I. (Magnetic Particles Inspection). On defect x.y.1 residual stresses in the dent are determined by X Rays at the surface and in several locations along the cross-section by neutron diffraction (NIST in USA and Chalk River Reactor Facility in Canada are kindly contributing these very involved neutron diffraction measurements).

Metallurgical and fracture investigation are performed after creation of defect x.y.1 and also after burst and fatigue tests to examine potential change of microstructure, presence of micro-cracks and to estimate experimentally levels of local strains in the dented and gouged areas. Table 4.2 summarizes all defect dimensions (**residual** dent depth at no pressure, gouge depth and length), and other characteristics, like internal pressure during pipe aggression, at 72% of actual yield pressure, except for the ~ 5% deep dents that could be created only with a lower pressure, worn teeth and a slower aggression speed.

Defect	Tooth	Aggression	Energy (J)	Pressure (bar)	Dent depth (%)	Gouge depth (%)	Gouge length (mm)
1.1.1b		D	3424	85	1.1	26.5	135
1.1.2	Cal44		4713	85	1.6	6.3	150
1.1.3			-	85	1.3	11.3	135
1.2.1b		D	5816	85	2.6	43.0	110
1.2.2	Esco		7676	85	2.6	34.2	115
1.2.3			6145	85	2.5	46.8	105
1.3.1		SD	34930	30	5.3	27.8	331
1.3.2	C481		28312	30	5.9	29.1	375
1.3.3			23973	30	6.1	20.2	321
2.1.1		D	7331	85	1.5	22.2	175
2.1.2	Cal44m		5912	85	1.6	18.9	200
2.1.3			4907	85	1.5	20.0	165
2.2.1		SD	33974	20	4.7	20.0	331
2.2.2	BEA		26726	20	5.2	16.7	353
2.2.3			C481	28412	20	5.3	21.1

Table 4.2: Characteristics of dent and gouge defects created in MD 4-1.

“SD” means Slower Dynamic aggression with a worn tooth and “D” Highly Dynamic aggression with a sharp new tooth. Defect created by “SD” is a long deep dent hence associated with higher defect creation energy.

Table 4.3 shows that the **burst pressure of these damaged pipes is very close to the burst pressure of flawless pipes** due to the high ductility of these modern pipes, the **only exception being defect 1.2.2** which is a **very severe gouge** (depth 34%) in a shallow dent (2.6% deep).

Defect	Failure Pressure (bar)	Theoretical failure of pipe body (Barlow's formula)	Comments	Defect	Pmin - Pmax (bar)	Number of cycles to failure	Comments
1.1.2	133.3	132.7 – 146.0 (UTS=512 MPa-563.2MPa)	Rupture outside of defect in pipe body (not in seamweld ERW)	1.1.3	45 bar – 85 bar	10869	Several interruptions of fatigue test
1.2.2	110.3	132.7-146.0	Rupture in defect	1.2.3	45 bar – 85 bar (0.38 – 0.73 YS)	5200	
1.3.2	130.9	132.7-146.0	Rupture in defect	1.3.3	53 bar – 93 bar (0.46 – 0.80 YS)	20494	Pressure loading above the window of bulging effect
2.1.2	185.1	185.4 – 204.0 (UTS=628 MPa-691 MPa)	Rupture in defect	2.1.3	88 bar – 128 bar (0.55 – 0.80 YS)	17700	Pressure max at 0.80 of current YS
2.2.2	193.5	185.4 - 204.0	Rupture in defect	2.2.3	20 bar – 60 bar (0.12 – 0.37 YS)	2007	Pressure loading in the window of bulging effect

Table 4.3: Results for Burst tests (left) and Fatigue tests (right)

The fatigue failure results exhibit a one order of magnitude range of number of cycles to failure: 2,007 to 20,494. One interesting observation is that a fatigue test in the pressure range of the dent bulging effect (see § 4.2) leads to rapid failure as a function of number of cycles, even if fatigue pressure levels are low compared to burst pressure. Defect 2.2.3 loaded in the pressure range 20 bar - 60 bar in the dent bulging window (created at 20 bar) fails ten times more rapidly than defect 1.3.3 created at 30 bar and loaded with the same 40 bar pressure range, but well above the dent bulging window, between 53 bar – 93 bar.

Metallurgical post-failure investigation shows that the dent creation by dynamic impact with new sharp excavator teeth induced severe damage in materials with presence of hard layers associated with micro-cracks at the gouge surface (Figure 4.1.b and 4.1.c).

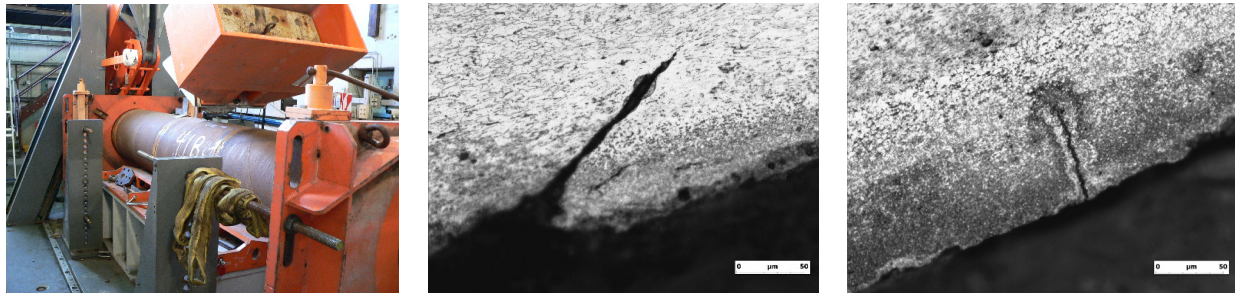


Figure 4.1: a) Pipe Aggression Rig; Presence at the gouge surface of defect 1.1.1b. of b) cracks and c) hard layers (tooth metal at the surface, and hardened pipe body metal beneath)

The following sub-chapters provide more insight on one hand on instrumentation to record the longitudinal dent profile evolution during the pressure increase to burst failure, and on the other hand, on the gouge opening evolution during the fatigue test with observation of the crack-initiation and leak at the gouge surface via camera monitoring of targets during the fatigue test.

4.2 Example of instrumented burst test and results

Figures 4.2 presents the specific instrumentation to record the evolution of the dent longitudinal profile during pressure increase for a burst test, thus providing a unique insight into the axial component of the dent re-rounding process. The change in shape due to re-rounding is evident in Fig. 4.2 (right).

The vertical displacement along the dent at each time during the pressure increase provides the pressure range for the bulging effect Figure 4.3, defect 1.3.2), defined by the largest displacement for a given pressure increase. The dent starts to spring back just above its creation pressure, in this case 30 bar, with large displacements (up to 15 mm over 10 bar). This detailed knowledge of the dent re-rounding behavior is a completely original feature of this study, and was used to set the pressure range for the fatigue tests 1.3.3 and 2.2.3, as discussed above: in one case, cycling in the dent re-rounding range (short fatigue life due to larger associated vertical displacements, see Fig. 4.3), in the other case, cycling well above the re-rounding range (long fatigue life, as vertical displacements are more limited, up to 2-3 mm for 10 bar, see Fig. 4.3).

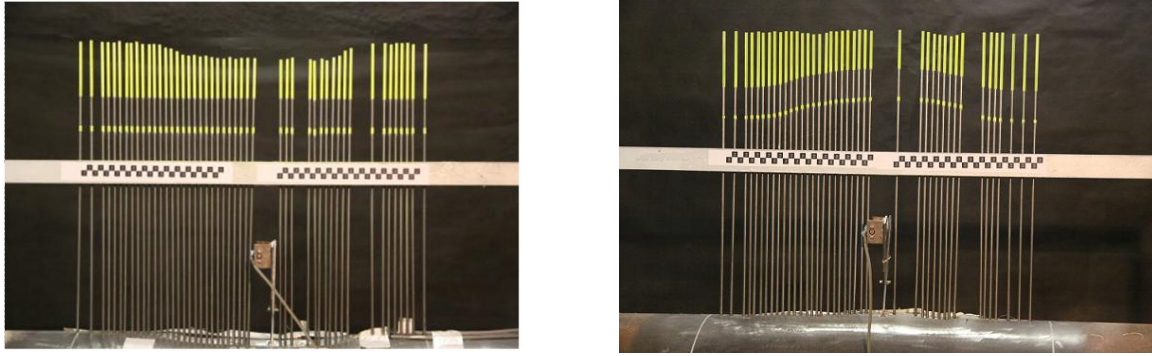


Figure 4.2: Longitudinal dent profile pressure=0 (left) and just before burst (right).

Internal Pressure during defect creation (bar):	30	Defect	1.3.2	Pipe	1
Burst Pressure (bar):	130,9			Diameter (mm)	609,6
				Thickness (mm)	7,9
				Grade	X52

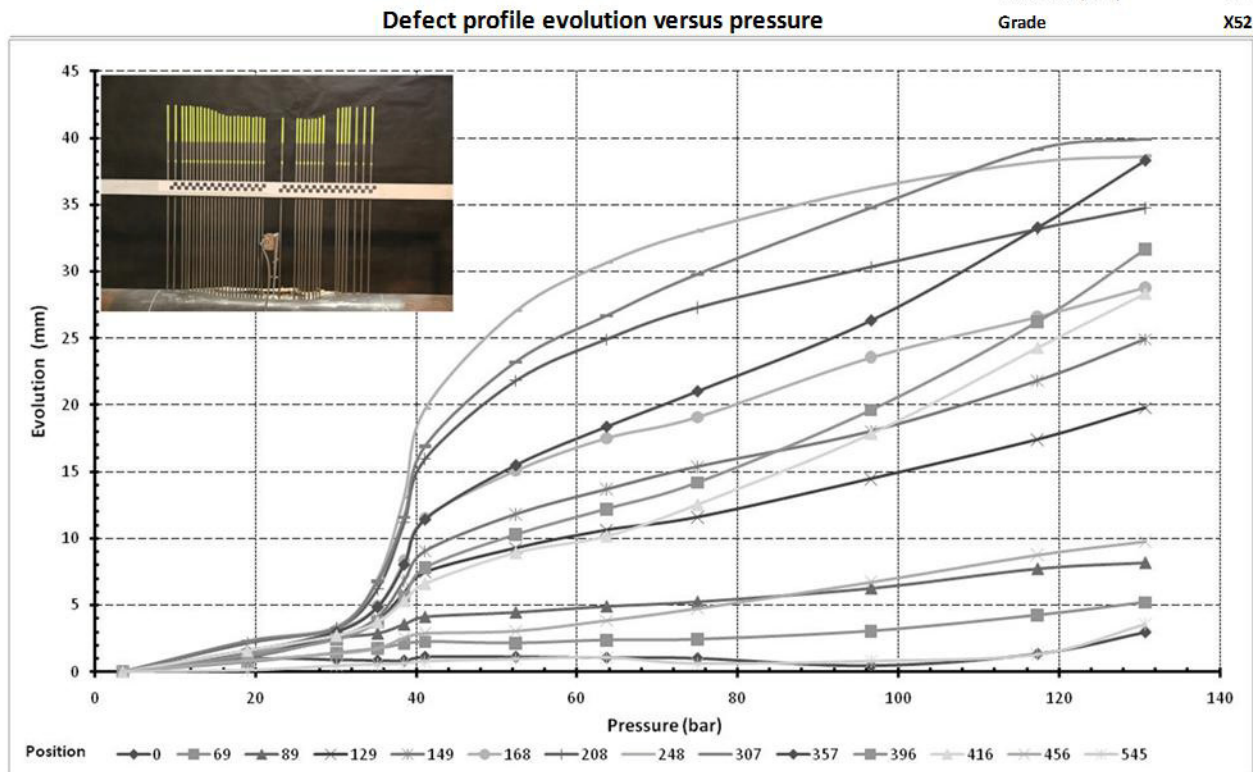


Figure 4.3: Evolution of dent profile versus pressure for defect 1.3.2 and identification of bulging above 30 bar, defect creation pressure.

4.3 Example of instrumented fatigue test and results

To determine the gouge opening evolution during the fatigue cycles and to capture more precisely the instants of crack-initiation and leak appearance, a camera associated with targets on each side of the gouge were installed (Figure 4.4). Pictures are taken at each maximum and minimum cycle pressures.

Figure 4.5 provides an evolution graph of targets displacement for defect 2.2.3, and photos when the crack initiation and leak appear at the gouge bottom. The evolution of the targets displacements follows that of the clip gauge opening displacement in a similar trend, with a larger amplitude. Slope changes are also more visible, hinting for initiation around 1200 cycles in this case.

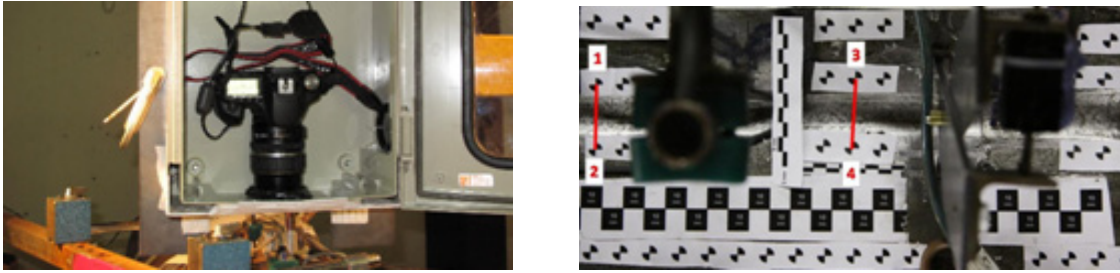


Figure 4.4: Camera (left) and target pairs 1-2 and 3-4 to follow the gouge opening displacement (right).

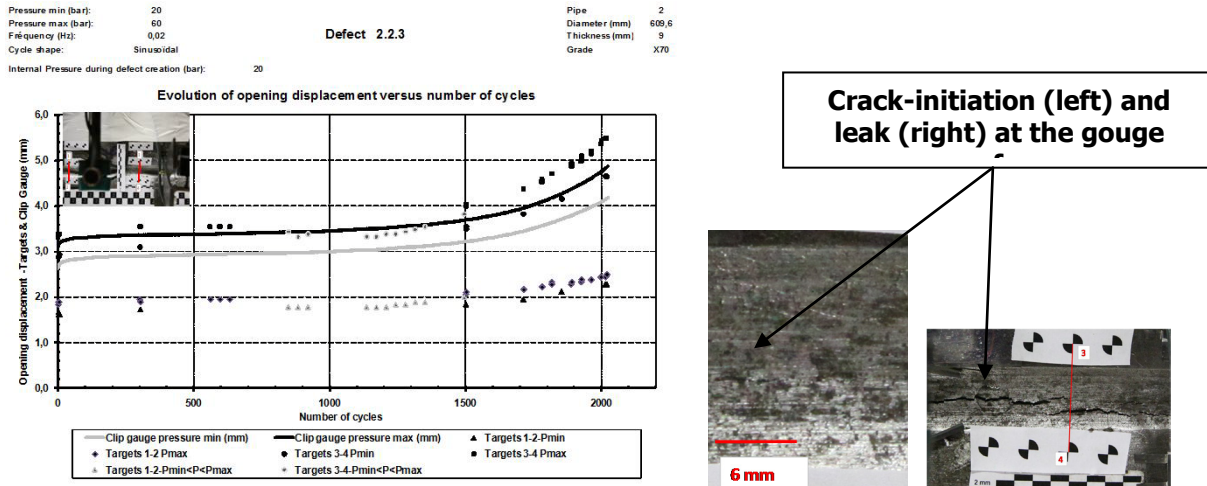


Figure 4.5: Evolution of targets displacement (black and grey symbols) and photo of crack-initiation and leak at the gouge surface.

5. CURRENT APPROACH IN FATIGUE MODELING FOR DENT AND GOUGE DEFECTS

5.1 Background for modeling approaches

In complement to the full-scale experimental work just detailed, the PRCI initiated a pair of independent modeling projects whose objectives were to assess 1) the immediate failure pressure a dent and gouge defect (MD-4-3), and 2) its potential for possible pressure-cycle induced fatigue crack growth (FCG) at damage that did not lead to immediate failure (MD-4-4).

Project MD-4-3 is not addressed here, so results on burst strength needed here to evaluate final defect dimensions after fatigue growth are provided based on prior developments that had shown success in predicting damage severity, which also a part of project PRCI PR3-9305 [10].

The concept for the MD4-4 approach was founded on the realization that if the dent and/or gouge, or local changes in steel properties diminish to zero, as could occur in a minor contact event, then the resulting circumstances are identical to the simple long-quantified case that involves an isolated crack in a damage-free pipe (e.g. [11], [12]). Because this approach adapts already proven technology for fracture and FCG in undamaged pipes, it is technically sound – as well as fiscally prudent. Conceptually, this mechanics/fracture framework quantifies the role of the dent and/or gouge in modifying the local stress-strain field, and accounts for other local changes like pre-strain on the properties to the extent required. Because of this basis in mechanics and fracture theory, MD4-4 could use this existing technology independently of MD4-3 to first predict combinations of failure pressure and damage size in terms of initial and final crack sizes, and then complete the fatigue predictions.

5.2 Immediate failure predictions – a first approach using existing information

The basic approach to predict flow and fracture behavior, as well as FCG at cracks in pipelines traces to the early 1970s. In that era, major investments in offshore structures for oil production, such as tubular template platforms [13], nuclear energy with its reliance on vessels and piping (e.g. [14]). Aspects of the structural and life-assessment technology developed then remain largely viable today for applications adequately quantified in terms of the LEFM, and its crack-driving force known as the stress-intensity factor, denoted K [15], with only minor differences emerging since. In contrast, major developments have emerged since then to address scenarios requiring nonlinear [elastic plastic, EP] fracture mechanics [16] (NLFM), and the use of J-based crack-driving force, as adapted for example to pipeline applications (e.g., [12]).

The only major uncertainty in the damage severity assessment framework developed in the PRCI PR3-9305 circa 2000 lay in quantifying the effects of re-rounding on the crack driving force, because while that work addressed this issue it did not do so adequately to quantify a generic solution [17]. For the present predictions, without the physically and geometrically nonlinear mechanics analysis done for the concerns of PR3-9305, differences in controlling factors like diameter, D , and diameter to thickness, D/t , and properties oblige the **use of experience-based trends developed for other cases**, and empirical inference in reference to the axial displacements reported earlier.

Experience also comes to bear observing that Project MD4-1 has burst and cycled dent and gouge damage that was created in quite high toughness pipe. Prior PRCI work involving burst testing of damage-free pipe has shown that quite long deep defects can survive to pressures the order of SMYS and above [17], just as reported earlier for the damage burst tests. It also has shown that defect failure response can be predicted [17], and that pipe properties [17] (geometry, yield stress, Y , ultimate stress, U , and fracture resistance expressed by CVN energy) discriminate whether failure will be collapse controlled versus fracture controlled. Such technology clearly indicates that for the pipe and test circumstances reported here collapse controls. Where collapse controls, quite high failure pressures can be anticipated because even though cracks form, the pipe toughness suffices to blunt the features. Blunt features fail like corrosion rather than sharp cracks, such that initiation of stable tearing and eventual growth and instability are deferred until quite high pressures. High pressures mean that re-rounding occurs well prior to failure, which can greatly simplify the analyses.

Using experience and empirical insight as just noted, the **technology framed in the context of PR3-9305** has been **used to predict the burst test outcomes for all testing reported here**. The same model, with the same properties has been used for each of the pipes, which is necessary to illustrate the predictive trends, and is justified by the fact that all pipes of a kind come from the same heat.

Figure 5.1 developed in reference to the approach of PR3-9305 shows on coordinates of pressure and defect length failure boundaries for the X52 pipe testing done in MD4-1. The contours shown in this figure represent defect depth, normalized relative to the wall thickness, and serve to quantify the final defect depth, a_f . Whether leak or rupture (LvsR) is predicted is dealt with by independent analyses, the scope of which is beyond the present paper. Comparable analyses have also been done for the X65 testing, but not included here due to save space.

As for the X52, the predictions summarized later for the X65 pipe have been based on the same model, with the same properties used for each of the X65 pipes.

It is evident from Figure 5.1 that the three results predicted for the X52 are rather good, in spite of this approach dating to circa 2000. In general the results are within the scatter evident in the pipe's mechanical properties.

Figure 5.2 summarizes the **predictions of failure pressure** corresponding to the **final defect depths**, with the predicted outcomes shown on the y-axis as a function of the actual failure pressure shown on the x-axis. It is apparent from this comparison that the predicted outcomes for all experiments correspond closely to the actual results, largely within a scatter-band comparable to the variability in the measured values of the UTS.

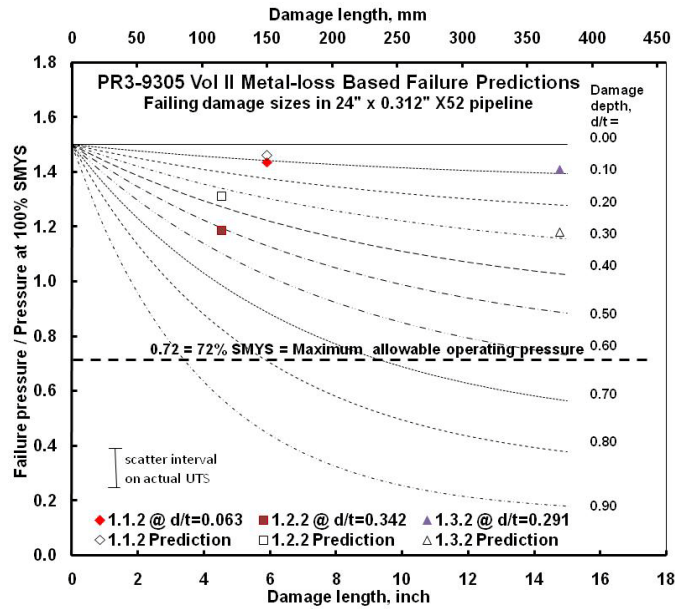


Figure 5.1. Predicted failure boundaries for MD 4-1 tests on X52

Such accurate outcomes serve to validate the predicted values of a_f that are used later in the FCG analyses.

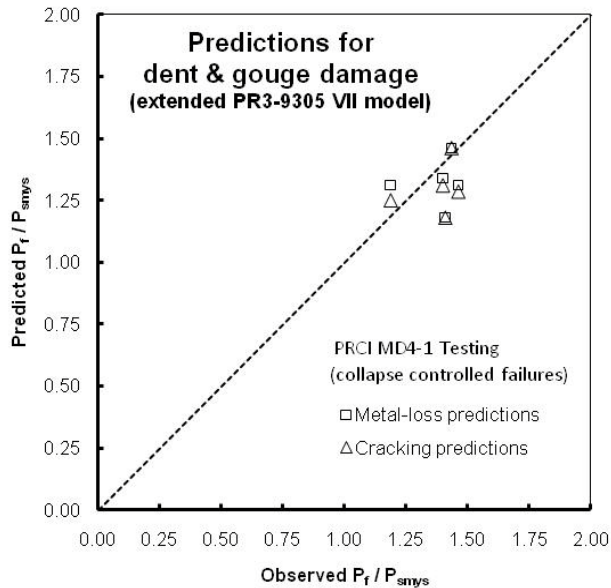


Figure 5.2 Comparing predicted with actual failure pressure (approach of PR3-9305 [10])

As suggested in view of the predicted outcome that plastic collapse controlled failure and the sizes of the damage features created for the testing in MD4-1, quite high failure pressures are predicted consistent with the observed results. While good predictions are evident, without more comprehensive parametric numerical analysis of re-rounding and its impacts on both the continuum concepts used to predict whether cracking initiates, and complementary fracture mechanics to address the onset of stable tearing and its growth, such models will remain research tools rather than transition into field-applicable technologies.

5.3 Fatigue failure predictions – a first approach using above information

Without geometrically and physically nonlinear FEA predicting fatigue response that can be sensitive to residual stresses, and involve exponents that range from 1/12 to 1/5 on initiation parameters, and from 3 to 4 on propagation parameters there is little hope for success.

Consider now initial outcomes from the FCG analysis. Absent the just noted detailed numerical modeling, and understanding of the transition in properties that forms in the layers that form below the damage implement, prediction of the potential population of initial crack sizes due to damage remain impractical. However, insight to quantify this population and whether depth suffices in lieu of lengths and depths follows from the literature and experience. Experience indicates that once the defect is long compared to its depth, its depth tends to dominate predicted life with little dependence on length. This tendency traces to the role of length and depth in quantifying the crack-driving force [15]. Lessons learned via LEFM FCG sensitivity studies done for critical nuclear piping in the late 1970s [19] provide further insight. Such trending indicates that four parameters control, including: the local stress range sensed by the crack tip; the threshold for growth including local closure and related issues; and the initial and final crack sizes. Each of these parameters has a central role in the efforts of MD4-4 thus far.

However, without clear characterization of re-rounding, and the influence of residual displacements, experience, the residual displacement fields at either end of the damage, and other of details developed must be used to offset uncertainties in the local crack driving force. As noted earlier, for the present this evolving need is being addressed as demands on the modeling become clear – with the scope of re-rounding effects and related complexity dealt with as circumstances dictate, with the least complexity for FCG beginning from a simple linear-elastic fracture mechanics (LEFM) construct.

Above the threshold for FCG, early work through the middle 1970s showed little effect of the steel type on the FCG rate[20], which is denoted da/dN , where da is the incremental FCG per cycle, and dN denotes the increment in number of cycles. With this nomenclature, the service life beyond incurring the damage is given in its simplest form by:

$$N = \int_{a_i}^{a_f} f(\Delta K) da \quad , \quad (E)$$

where ΔK is the range of K determined from the pipeline's operating conditions, a_i is the depth of the cracking due to damage, and a_f is the final depth that comes from results like that in Figure 5.1.

While the final crack depth parameter a_f as dealt with in PR3-9305 was generated in terms of toughness controlled failure because that work focused on lower-toughness steels, the very high toughness of the steels in MD4-1 means that Figure 5.1 reflects collapse controlled failure at metal-loss features. For this reason, the outcomes in Figure 5.1, and those summarized in Figure 5.2 have been assessed as metal loss using criteria developed and validated in the context of plastic collapse, such as PCORRC^(k), with recourse taken if needed to the prediction scheme for cracking and local strain at dents and gouges as detailed in PR3-9305 [10]. Based on that work, the value of a_f is equal to either the critical depth when rupture is predicated, or to the remaining wall thickness when a leak is predicated.

As indicated above the approach builds from the simplest formulation and address complexities in the crack driving force and other parameters as dictated by the outcomes. As such, Equation E has been evaluated for the nominal pressure histories used in the fatigue testing done as part of MD4-1, and reported earlier in this paper. It is broadly recognized that once a crack grows beyond a stress gradient that originates it, the crack driving force for continued growth quickly transitions to a form that ignores that gradient [15], and absent closure concerns also is independent of the wake of its growth [15]. This means that **once the crack has grown marginally into the pipe** below the damaged material at the gouge, its response can be quantified by that of a crack in a damage-free pipe, with the **depth of that crack quantified relative to the original wall thickness** – not the bottom of the gouge.

Given the actual damage depths imposed in MD4-1 ranged from about 6 to 35% of the wall thickness, and adding to that microcracking the order of about 0.1 mm, the initial crack depths is determined to range from about 0.6 mm up through about 2.8 mm. Because without microcrack initiation at the base of the

gouge there is only the blunt bottom of the gouge, without fatigue crack initiation continued FCG or stable tearing only can occur if microcracking is indicated upon re-rounding. Indicators of initiation include empirical data where full-scale testing is done, as for this paper, as well as analytically [10]. Cross-sections through damage made in field-failure analyses, as well as for simulated damage as in this paper have been made since the late 1970s that show several stages of cracking depending on the damage state. Quite shallow (micro) cracks have been observed that depending on the circumstances lay in deposited material, or in a work-hardened possibly transformed microstructure. In other circumstances, deeper but stable cracks have been observed that carry into a transition layer from the states just noted into the base structure of the line pipe, which in the limit breaches the wall leading to immediate failure. While as yet unproven by detailed measurements, because the hardened layer has much reduced toughness as compared to the base pipe for almost any line-pipe steel, three potential delayed failure states have been suggested to form upon re-rounding [10]:

1. No significant cracking in the hardened or transformed layer (which precludes cracking into the base pipe steel), was asserted to be benign for historic gas-transmission service
2. Involving cracking into the low-toughness hardened layer, with the suggestion that it likely continued through its full depth and then quickly arrested in the tougher base pipe
3. Cracking that continues into the base pipe that remained stable at the re-rounding pressure.

As dictated by fracture mechanics, the cracking depth into the hardened layer or into the base pipe depends on the pipe's toughness, and the severity of the crack-driving force [15]. Because the toughness in the hardened layer is low, and the response likely quite brittle if the steel transforms to un-tempered martensite, cracks nucleating in that layer are very likely to grow unstably through the layer's full thickness. Once into the base pipe, because the toughness there depends on the vintage and the chemistry and processing involved in its production, the **range of continued crack responses depends broadly on the pipe involved rather than the damage state**. This can lead to **significant variability in cracking behavior**, which some might misconstrue as scatter, or poor quality data. Further on such cracking is noted in References [15] and [17].

Based on the just-noted construct, Figure 5.3 illustrates results of predicted crack-growth for Test 1.1.3, as reported earlier in this paper, for initial total crack depths set at 0.99, 1.30, and 1.52 mm. These results reasonably characterize typical predictive trends. The y-axis in this figure indicates crack depth below the pipe's surface, as noted above, rather than the depth below the gouge, while the x-axis is the number of applied cycles. The deeper microcracks developed for Test 1.1.3 grew through the hardened damage layer arresting quickly due to the tough base pipe, being reported earlier in the paper the order of 0.1 mm deep prior to cycling, with related evidence indicating depths up to twice that. When the microcrack depth of 0.1 mm is added to the physical gouge depth as the basis to predict FCG, the initial total depth for Test 1.1.3 is 0.99 mm (referenced to the original outer surface of the pipe). The LEFM crack-driving force "K" used that value of a_i , and considered the crack to be shallow compared to its length but excluded the effect of the plastic zone. The value of K was based on the nominal pressure cycling, and included both membrane tension and local bending effects. Accordingly, the value of K had a form comparable to that adopted by Hopkins circa 1982⁽¹⁾, except for excluding the plastic zone correction.

Sensitivity studies indicate that including a plastic zone correction does affect a non trivial reduction in life, but its effect is small compared to the effect of initial depth. The predicted life corresponding to $a_i = 0.99$ mm found to be 34,888 cycles compares reasonably with the actual life of 10,869 given the scatter usual in fatigue testing.

Results shown in Figure 5.3 clearly show the **significance of the initial total crack depth**, as just more than a 50% increase in depth causes an almost 13-fold decrease in fatigue life. Thus, it is clear that this **parameter must be well characterized** if useful results are to be obtained. It is also apparent that if the initial size is accounted for the final size has much less influence, although this is not always the case.

While as the form of Equation E shows there is more involved than initial crack size, the strong dependence on initial depth coupled with the range of initial depths from 0.6 mm up through about 2.8 mm

suggests a significant range of fatigue lives is anticipated, and indeed observed. While such a range of lives is consistent with expectations, detailed evaluation of the fatigue lives observed it arises more due to the unique nature of the re-rounding than is adequately represented using the specific model used here, or a variation that assesses cracking referenced to the root of the damage.

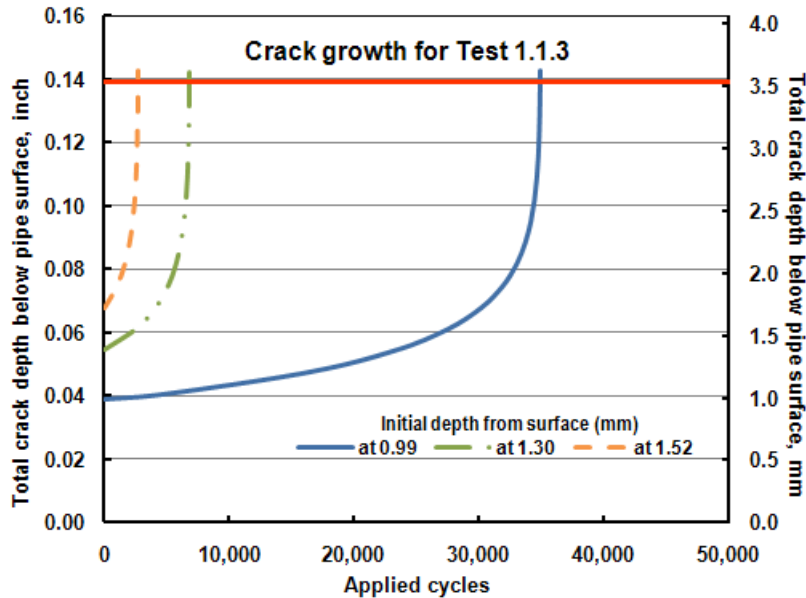


Figure 5.3 Predicted cycle-dependent growth

Figure 5.3 would be an acceptable predictive outcome based on what is a relatively simple model if the initial crack sizes as the contact was released and the damage re-rounded broadly predicted the number of cycles to grow the crack to a critical size as observed in the full-scale testing. While as noted above a wide range of predicted lives was predicted consistent with expectations in terms of initial defect depth and nominal stress range, the sequence of the shortest to longest life is somewhat out of sync with mix of damage depths and effective local pressure cycles. As such, this simple model adopted fails to capture the key aspects of fatigue crack growth from the damage for the pressure histories imposed. Moreover, there is a tendency to slightly over-predict life, although this easily can be offset by slightly larger initial crack depths.

Consideration of the literature indicates several plausible factors all of which lead to accelerated FCG rates, and so to shorter lives – the inclusion of one or more of which could be necessary if the micro-crack depth considered reflects the worst-case in the depth population. Analysis of the region of and also below the damage also indicates the presence of notches or grooves as origins for cracks, while the ductility of the steel involved would support a plastic zone whose size is dictated by the geometry of damage and the magnitude of the local stress [10]. While experience suggests this is unlikely a major driver, it is known that the growth of cracks in inelastic notch fields [23] cannot be simply predicted by LEFM or NLFM unless the unique local fields and crack closure are addressed [26 - 27]. Re-rounding also leads to a magnified local stress field relative to the nominal cycling considered to this point [10], with the displacements measured in the full-scale testing suggest is most critical.

Work continues to evaluate modeling options, including work to parametrically quantify the effects of re-rounding, and to better understand the extreme-value population of initial defect sizes if the correct form of crack driving force is to be identified.

6. CONCLUSION

As a summary, the present paper developed two aspects related to improving our fundamental knowledge about the failure mechanisms of dent and gouge defects.

Experimentally, several outcomes concerning modern, tough steels were established on a database of 15 tests:

- Highly dynamic impact leads to the creation of a **very hard superficial layer** containing tooth material, and very prone to micro-cracking; its limited thickness – 100 to 200 µm deep – confines these micro-cracks above a strain –hardened layer; more investigations will be performed also on the deep dents with a less quick aggression
- For modern clean and very tough steels, **moderate dent and gouge damage does not affect significantly the pipe's burst strength**; Severe gouging was found to be the only case of significant drop in burst pressure below the flawless pipe
- For **deeper dents**, ~5% residual depth, for which the re-rounding process involves larger displacements above the internal pressure during denting, there is a strong influence of the mean level of the pressure cycling range: if this is immediately above the pressure during denting, a large cyclic re-rounding will lead to a short fatigue life; conversely, if the pressure range is well above the dent pop-up pressure range, then the fatigue life will be longer, a displacements will be smaller. This finding has not been verified on shallower dents yet, as it used a novel measurement technique.
- A **first fatigue modeling approach** showed that, based on limited data, **it is possible to characterize the fatigue response** of line pipe damaged by dents and gouges, but it is clear that this requires a viable assessment of the initial depth of the cracking, and can in some pressure-contact circumstances require an understanding of the local effects of re-rounding in the wake of the damage implement.

Experimental work will go on with finishing metallurgical characterizations and undertaking a similar work on two different vintage pipes, that will add more defects: 12 = 4 cases * 3 defects / case to the reference data-base.

Modeling work will focus on better quantifying the local re-rounding and its influence on the stress-cycle experienced at the crack. Once this is complete, if needed the work will more broadly consider other local nonlinearities.

The final outcome of the expected knowledge improvements about the mechanical strength of dent and gouge combinations will be applicable by pipeline operators, in order to enhance safety for the general public as well as operating personnel.

7. ACKNOWLEDGMENTS: The authors hereby acknowledge the funding received from PRCI and DOT to pursue this work on dent and gouge mechanical strength, and the international coordination with EPRG. All individuals that contributed valuable work via the PRCI project teams, or the DOT project team, and in the two contractors' teams should also receive our recognition.

8. REFERENCES

- 1 Anon. (December 2008) 1970 – 2007 Gas Pipeline Incidents 7th Report of the European Gas Pipeline Incident Group. www.egig.eu
- 2 Anon. (2011) All reported gas transmission pipeline incidents. Interpretation by the authors. <http://primis.phmsa.dot.gov/comm/reports/safety/>
- 3 B.N. Leis, R.B. Francini (1999) Line Pipe Resistance to Outside Force. Volume 2, Assessing Serviceability of Mechanical Damage, PR-3-9305, Catalog L51832, PRCI, Battelle Memorial Institute.

- 4 Chang-Kyung Oh, Yun-Jae Kim, Jong-Hyun Baek, Young-Pyo Kim and Woosik Kim. (2007) A phenomenological model of ductile fracture for API X65 steel. *International Journal of Mechanical Sciences*, 49, p1399-1412.
- 5 Noaki Fukuda, Naoto Hagiwara, Tomoki Masuda. (2002) Effect of prestrain on tensile and fracture toughness properties of line pipes. 4th International Pipeline Conference, September 29-October 3.
- 6 Hai Qiu, Manabu Enoki, Kazuo Hiraoka and Teruo, Kishi. (2005) Effect of prestrain on fracture toughness of ductile structural steels under static and dynamic loading. *Engineering Fracture Mechanics*, 72, pp 1624-1633.
- 7 Marshall, P. W., (1979) Strategy for Monitoring, Inspection and Repair for Fixed Offshore Platforms. in "Structural Integrity Technology," ASME. pp. 97-110
- 8 Yukawa, S., '1979) ASME Nuclear Code Applications of Structural Integrity and Flaw Evaluation Methodology. in "Structural Integrity Technology," ASME, pp. 29-38.
- 7 Leis, B. N., Mayfield, M. E., Forte, T. P., and Eiber, R. J. (1980) Influence of Initial Defect Distribution on the Life of the Cold Leg Piping System. in Mechanics of Nondestructive Testing, Plenum Press, , pp. 325-342.
- 8 Bolton, B, Semiga V., Tiku, S. Dinovitzer, A. And Zhou, J. (2010) Full Scale Cyclic Fatigue Testing of Dented Pipelines and Development of a Validated Dented Pipe Finite Element Model. Proceedings of the 8th international Pipeline Conference, IPC2010-31579.
- 9 Anon., (2009) ANSYS 11.0 Reference Manual, ANSYS Inc.
- 10 Leis, B. N. and Francini, R. B. (2000) Line Pipe Resistance to Outside Force – Volume II: Assessing Serviceability of Mechanical Damage. PRCI Report PR3-9305.
- 11 Kiefner, J. F., Maxey, W. A., Eiber, R. J., and Duffy, A. R. (1973) Failure Stress Levels of Flaws in Pressurized Cylinders. *Progress in Flaw Growth and Fracture Testing*, ASTM STP 536. pp. 461-481.
- 12 Leis, B. N., Brust, F. W., and Scott, P. M. (June 1991) Development and Validation of a Ductile Flaw Growth Analysis for Gas Transmission Line Pipe. PRCI Catalog No. L51543, Pipeline Research Council International.
- 13 Marshall, P. W. (1979) Strategy for Monitoring, Inspection and Repair for Fixed Offshore Platforms. in *Structural Integrity Technology*, ASME, pp. 97-110.
- 14 Yukawa, S., (1979) ASME Nuclear Code Applications of Structural Integrity and Flaw Evaluation Methodology. in *Structural Integrity Technology*, ASME. pp. 29-38.
- 15 Broek, D. (1974) *Engineering Fracture Mechanics*, Nordhoff.
- 16 Kanninen, M. F. and Popelar, C. H. (1986) *Advanced Fracture Mechanics*, Oxford.
- 17 Leis, B. N. and Hopkins, P. (2004) Mechanical Damage Gaps Analysis. in Volume I -Pipeline Technology, Science Surveys Ltd. pp 1921 – 1943; but most complete as (2002) PRCI Report PR3-0277. PRCI Cat L52013.
- 18 Leis, B. N., (2001) Hydrostatic Testing Of Transmission Pipelines: When It Is Beneficial and Alternatives When It Is Not. PRCI Report PR-3-9523, Pipeline Research Council International: see also Olson, R. J., Narendran, V. K., Leis, B. N., Kilinski, T. J., Scott, P. M., and Gertler, R. C. "Full-Scale Testing to Validate PAFFC and Develop Data to Assist Evaluating the Benefits of Hydrotesting", Appendix 7 of this report.
- 19 Leis, B. N., Mayfield, M. E., Forte, T. P., and Eiber, R. J. (1980) Influence of Initial Defect Distribution on the Life of the Cold Leg Piping System," in *Mechanics of Nondestructive Testing*, Plenum Press. pp. 325-342.

- 20 Rolfe, S. T. and Barsom. (1977) J. M., Fracture and Fatigue Control in Structures, Prentice-Hall.
- 21 Stephens, D.R., Leis, B.N., Kurre, J.D., and Rudland, D.L., January (1999) Development of an Alternative Failure Criterion for Residual Strength of Corrosion Defects in Moderate- to High-Toughness Pipe. PRCI Cat. No. L51794,.
- 22 Hopkins, P. and Carins, A., (1981) A Fracture Model to Predict the Failure of Defects in Dented Line Pipe. British Gas, EPRS R2382.
- 23 Leis, B. N. (1985) Displacement Controlled Fatigue Crack Growth in Inelastic Notch Fields: Implications for Short Cracks. Engineering Fracture Mechanics, Vol. 22, No. 2 pp. 279-293: see also Gowda, C.V.B., Topper, T. H., and Leis, B. N. (1972) Crack Initiation and Propagation in Notched Plates Subject to Cyclic Inelastic Strains", International Conference on Mechanical Behavior of Materials, Kyoto, Japan, Vol. II. pp. 187-198.
- 24 Leis, B. N., Kanninen, M. F., Hopper, A. T., Ahmad, J., and Broek, D., (1986) Critical Review of the Fatigue Growth of Short Cracks. Engineering Fracture Mechanics, Vol. 23, No. 5. pp. 883-896.
- 25 Kanninen, M. F., Ahmad, J., and Leis, B. N., (1981) A CTOD-Based Fracture Mechanics Approach to the Short Crack Problem in Fatigue. Mechanics of Fatigue. AMD/ASME, AMD-Vol. 47. pp. 81-96.
- 26 Anon. (1983) Short Crack Effect in Airframe, Materials, and Components, Advisory Group on Aeronautical Research and Development Panel Report--Behavior of Short Cracks in Airframe Components. AGARD CP 328.
- 27 Hahn, G. T., Sarrate, M. and Rosenfield, A.R. (1969) Criteria for Crack Extension in Cylindrical Pressure Vessels. *I J Frac Mech*, Vol.5 pp. 187-210.